Clinical Endocrinology (2013) 78, 957–965 doi: 10.1111/cen.12054

ORIGINAL ARTICLE

# A report of two novel *NR5A1* mutation families: possible clinical phenotype of psychiatric symptoms of anxiety and/or depression

Ayuko S. Suwanai*, Tomohiro Ishii*, Hidenori Harunat, Atsuyuki Yamataka‡, Satoshi Narumi*, Ryuji Fukuzawa§, Tsutomu Ogata¶,** and Tomonobu Hasegawa*

*Department of Pediatrics, Keio University School of Medicine, †Department of Pediatrics and Adolescent Medicine, ‡Department of Pediatric General and Urogenital Surgery, Juntendo University School of Medicine, §Department of Pathology, Tokyo Metropolitan Children's Medical Center, ¶Department of Molecular Endocrinology, National Medical Center for Children and Mothers Research Institute, Tokyo, Japan and **Department of Pediatrics, Hamamatsu University School of Medicine, Shizuoka, Japan

## Summary

**Objective** NR5A1 or steroidogenic factor 1 is a nuclear receptor that plays important roles in the hypothalamus–pituitary–steroidogenic axis. The clinical phenotype of most 46,XY mutation carriers includes disorders of sex development (DSD) without adrenal insufficiency, whereas 46,XX mutation carriers have phenotypes ranging from no symptoms to ovarian insufficiency. Although genetically engineered ventromedial hypothalamus-specific *Nr5a1* knockout mice show anxiety behaviour, no psychiatric symptoms have been reported in human *NR5A1* mutation carriers. We report clinical and molecular findings for individuals (from two families) with *NR5A1* mutations, showing psychiatric symptoms.

**Design and methods** We screened for *NR5A1* mutations in a cohort of 34 patients with 46,XY DSD using PCR-based sequencing. Psychiatric symptoms were assessed using mental health assessment tools and structured clinical interviews. Functional properties of detected mutant *NR5A1*s were studied *in silico* and *in vitro*, including three-dimensional (3D) mutation models, subcellular NR5A1 protein localization and transactivation assays.

**Results** We found 2 (46,XY) patients with *NR5A1* heterozygous novel mutations (p.D257fs and p.V424del), which were transmitted from their respective mothers. The patients' clinical findings indicated DSD without adrenal insufficiency. Both mothers showed psychiatric symptoms, including excessive anxiety and/or depression. The mother and grandmother of one patient had premature ovarian insufficiency. Functional studies showed altered 3D models of p.V424del and normal subcellular NR5A1 localization and impaired transcriptional activation without dominant-negative effects in both mutations.

**Conclusions** We found 2 (46,XX) *NR5A1* mutation carriers with excessive anxiety and/or depression. These results suggest that excessive anxiety and/or depression are possible clinical phenotypes of 46,XX *NR5A1* mutations.

(Received 25 July 2012; returned for revision 9 August 2012; finally revised 28 August 2012; accepted 3 September 2012)

## Introduction

NR5A1 (steroidogenic factor 1 [SF1] and AD4BP/FTZF1) is a nuclear receptor expressed in the gonad, adrenal cortex, anterior pituitary, hypothalamus and spleen.[1] NR5A1 plays crucial roles in adrenal and gonadal development, expression of pituitary gonadotrophins and development of the ventromedial hypothalamus (VMH).

Genetically engineered *Nr5a1*-deficient ($Nr5a1^{-/-}$) mice have agenesis of the adrenal glands and gonads, impaired function of pituitary gonadotrophs and VMH abnormalities.[1,2] To define the role of NR5A1 in each tissue, pituitary, VMH and gonadal-specific knockout mice were generated.[2,3]

In humans, the clinical phenotype of most 46,XY mutation carriers is of disorders of sex development (DSD) without adrenal insufficiency. A wide phenotypic spectrum exists in XY DSD subjects, ranging from complete testicular dysgenesis leading to female assignment to severe penoscrotal hypospadias leading to male assignment. The clinical phenotype of 46,XX mutation carriers ranges from no symptoms to ovarian insufficiency.[4] While these gonadal phenotypes have been well described, other phenotypes of *NR5A1* mutations in humans remained unclear. For example, loss of *NR5A1* function in the VMH in humans might cause obesity. Another possibility is anxiety-like behaviour, which has been observed in VMH-specific $Nr5a1^{-/-}$ mice, although no human mutation carrier with psychiatric symptoms has been reported.

Herein, we report two families carrying novel *NR5A1* mutations by screening 34 cases of Japanese 46,XY DSD. We characterized the functional effects of these mutations and evaluated psychiatric symptoms in the affected families.

Correspondence: Tomonobu Hasegawa, Department of Pediatrics, Keio University School of Medicine, 35 Shinanomachi, Shinjuku-ku, Tokyo 160-8582, Japan. Tel.: 81333531211; Fax: 813 53791978; E-mail: thaseg@a6.keio.jp

## Patients and methods

### *Patient report*

We enroled 34 Japanese patients with 46,XY DSD with varying degrees of hypospadias (Table 1).

*Family 1 (Fig.1a. left).* The proband (a 12-year-old female; II-6, Proband 1) was born to nonconsanguineous parents after an uncomplicated pregnancy and delivery (Fig. 1a). Ambiguous genitalia were noticed at birth by obstetricians, and the legal gender was assigned as female. At 9 months of age, clitoromegaly without labial fusion was observed (Fig. 1b). The vaginal and urethral orifices were separated. Small masses were palpable in the labia majora bilaterally. There was no skin hyperpigmentation. Her karyotype was 46,XY. At 13 months of age, the external genitalia showed clitoromegaly (width: 12 mm, length: 15 mm; age-matched Japanese width and length of clitoris; 4·1 ± 1·1 and 4·7 ± 1·1 mm, respectively).[5] Pelvic MRI showed a markedly hypoplastic vagina, and no ovaries or uterus were present. A GnRH stimulation test resulted in LH and FSH peaks of 3·2 and 7·2 U/l, respectively (IFMA, reference value of LH and FSH peak ranges in prepubertal males under 10 years: 1·70–3·77 and 4·38–9·48 U/l, respectively).[6] The basal testosterone concentration was 3·12 nmol/l; after HCG stimulation (3 000 IU/m$^2$ intramuscularly daily for 3 days), it was increased to 7·32 nmol/l (the basal and stimulated testosterone concentrations following daily injections of 2 000 IU HCG in healthy males aged 5·5–9 years at Tanner stage 1 are 0·62 ± 0·14 and 6·00 ± 0·94 nmol/l, respectively.[7]) Gonadectomy was performed after

**Table 1.** Phenotypes and genotypes of six subjects with mutations in the *NR5A1* gene

| Variable | Family 1 | | | Family 2 | | |
|---|---|---|---|---|---|---|
| *NR5A1* genotype | D257TfsX39 (heterozygous) | | | V424del (heterozygous) | | |
| | III-6 | II-4 | I-2 | III-4 | II-3 | III-1 |
| Social sex | Female | Female | Female | Male | Female | Female |
| Karyotype | 46,XY | 46,XX | 46,XX | 46,XY | 46,XX | 46,XX |
| Age at last visit (year) | 13 | 40 | 73 | 6 | 46 | 9 |
| Manifestations | Hypospadia (urogenital sinus) Clitoromegaly Testes in bilateral labia | POI | POI Menopause at 38 years Osteoporosis at 62 years | Hypospadia (penoscrotal) Micropenis Separated scrotum Small testes Enlarged prostatic utricle | Normal | Normal at present |
| Age at endocrinological examination (year) | 1 | 37 | | 3 | | |
| LH/FSH | | | | | | |
| Baseline | 0·2/0·3 | 44·1/77·8 | ND | <0·1/2·0 | ND | ND |
| GnRH stimulated | 3·2/7·2 | ND | | 1·7/18·1 | | |
| Basal E2 (nmol/l) | 73·4 | 77·1 | ND | 29·4 | ND | ND |
| Testosterone( nmol/l) | | | | | | |
| Baseline | 3·12 | <0·05 | ND | 0·17 | ND | ND |
| HCG stimulated | 7·32 | ND | | 1·2 | | |
| Psychiatric manifestations | Withdrawn* | Severe depression† Anxiety and depression‡ | ND | Anxiety/ Depressed* Aggressive* | Moderate depression† | ND |

*Assessed by the Child Behaviour Checklist (CBCL).
†Assessed by the Beck Depression Inventory (BDI)-II.
‡Diagnosed by the Structured Clinical Interview for DSM-IV Axis Disorders (SCID).
POI, premature ovarian insufficiency; ND, not determined, no data; E2, estradiol.
Reference values.
Baseline ranges in boys, aged 1 year: LH, 0·04–0·77 U/l, FSH 0·18–2·06 U/l; aged 3 years: LH, 0·02–0·46 U/l, FSH, 0·2–2·32 U/l as observed using immunofluorometric assay (IFMA) (45).
Stimulated ranges in prepubertal boys, under 10 years: LH, 1·70–3·77, FSH, 4·38–9·48 U/l (IFMA) (12).
Baseline range of after menopause: LH, 11–50, FSH 26–120 U/l, E2 <77·1 nmol/l, progesterone <1·3 nmol/l as observed using electrochemiluminescence immunoassay (ECLIA) (14).
The basal and response testosterone concentrations following daily injections of 2000 IU HCG in healthy boys aged 5·5–9 years at Tanner stage 1; 0·62 ± 0·14 and 6·00 ± 0·94 nmol/l, respectively (14).

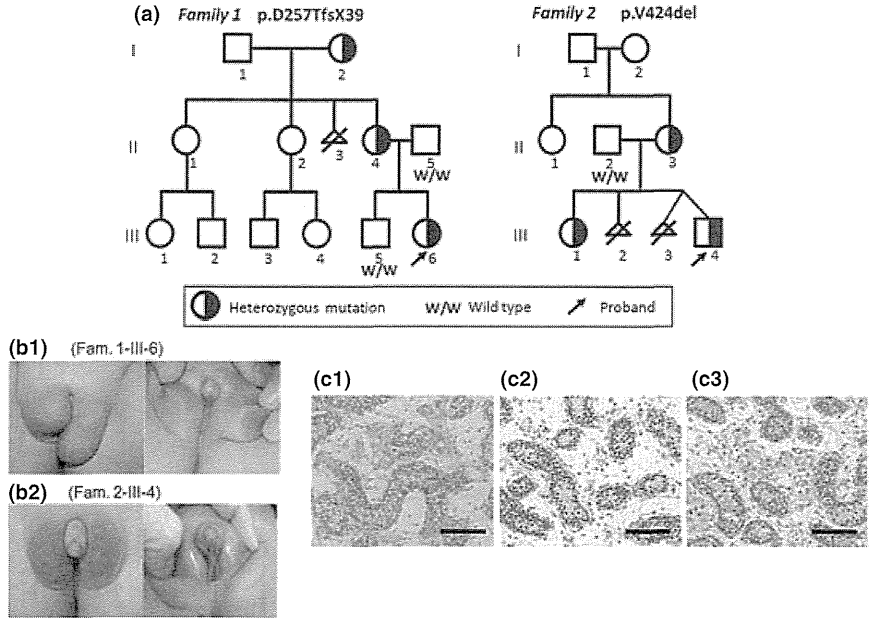


**Fig. 1** Pedigrees of two families with 46,XY disorders of sex development and histological analysis of samples from Proband 1. (a) Pedigrees of two families with *NR5A1* mutations. Squares represent male family members and circles represent female family members. Half-solid squares and circles represent carriers of the mutation. Triangles represent miscarriages and deceased twin. The index patient is indicated with an arrow in each family. The genotypes of the parents and siblings of the proband were determined by molecular analysis. (b) Genital features of the probands. Left panel: Proband of Family 1. Right panel: Proband of Family 2. (c. c-1) Gonadal histological analysis (the bar represents 100 $\mu$m, H&E) of the Proband 1 shows the small size and decreased numbers of seminiferous tubules (the diameter of the seminiferous tubules: 63·6 $\mu$m; age-matched control diameter: 77·4 ± 2·1 $\mu$m; the number of the seminiferous tubules was 30–34 tubules/0·64 mm$^2$; age-matched control: 77·4 ± 2·1 tubules/mm$^2$) and decreased spermatogonia (the number of spermatogonia per 10 tubular cross-sections is 7–9 and that per 100 Sertoli cells was 3; age-matched control: 13·3 ± 1·3 and 5·9, respectively). The number of Sertoli cells was high (mean, 33 per 10 tubules; age-matched control: 22·2 ± 0·3). Occasionally, foci of aggregated Leydig cells were observed. No Müllerian derivatives could be identified. Gonadoblastoma was not present. (c-2) Immunostaining for wild type (WT)1. Nuclear accumulation of WT1 is restricted to the Sertoli cells. (c-3) Immunostaining for Ad4BP/SF1. Ad4BP/SF1 localized to the nuclei of the Sertoli cells and Leydig cells. The staining intensity of Ad4BP/SF1 varied among the cells.

these stimulation tests. An ACTH stimulation test was normal (data not shown). We initiated oestrogen replacement therapy at 11 years of age. The patient has never had any suspected episodes of adrenal crisis. At present, she attends elementary school as a girl; reportedly, she has had no trouble in her school life.

The mother of the proband (a 38-year-old female; II-4) has normal body proportions and body mass index of 18·8 kg/m$^2$. Physical examination was unremarkable. Her menarche was at 14 years of age. She became pregnant spontaneously without any fertility treatment and delivered when she was 27 and 28 years old. Her menstrual cycle was regular and 30 days in length (healthy cycle of Japanese women: once per 25–38 days; variation of the interval between menses: <7 days), and the duration of her menstrual bleeding was 2–7 days, although the flow was scanty (duration of healthy menstrual bleeding: 3–7 days; volume: 20–80 ml) until the age of 30 years. Since her early 30s, the duration was less than 2 days. She has always felt anxious, fatigued and unmotivated. She consulted a psychiatrist about these mental health problems, and Clonazepam was prescribed. After she was 36 years old, her menstrual cycles were from 90 to 180 days in length. At 38 years of age, endocrinological assessment showed basal LH 44·1, FSH 77·8 U/l, E2 77·1 nmol/l and progesterone 0·64 nmol/l (ECLIA, reference values after menopause for LH, FSH, E2 and progesterone: 11–50U/l, 26–120 U/l, <77·1 nmol/l and <1·3 nmol/l, respectively).[8] She was diagnosed as having premature ovarian insufficiency by Anasti's criteria,[9] and hormone replacement therapy was initiated. Since the age of 38, she has suffered from irritable bowel syndrome. She has never had a history of obesity or emaciation. She has never had any episode of suspected adrenal crisis.

The maternal grandmother of the proband (I-2) was not obese and entered menopause when she was 38 years old. At the age of 62 years, she was diagnosed with osteoporosis.

*Family 2 (Fig.1a. right).* The proband (a 6-year-old boy; Fig. 1, III-4, Proband 2) was born to nonconsanguineous parents at full term (Fig. 1a). Ambiguous genitalia was noticed by obstetricians at birth. He had a small penis (stretched penile length of 15 mm; age-matched control length: 27·6 ± 3·6 mm),[10] small testes (volumes less than 1 ml, in the scrotum; age-matched control volumes: 1–2 ml),[11] penoscrotal hypospadias, bifid scrotum and an enlarged prostatic utricle that opened below the urethral meatus (Fig. 1b). No skin hyperpigmentation was observed. The karyotype was 46,XY, and the patient was raised as a boy. At 3 years of age, a GnRH stimulation test showed LH

and FSH peaks of 1·7 and 18·1 U/l. The basal testosterone concentration was 0·17 nmol/l and, after stimulation, increased to 1·2 nmol/l. ACTH stimulation test was normal (data not shown). At 3 years of age, urethroplasty was performed. No adrenal crisis occurred during surgery.

The mother of the proband (a 46-year-old woman; II-3) had an unremarkable medical history and physical examination. She developed menarche at 13 years of age. She gave birth spontaneously when she was 32 and 40 years old. Her menstrual cycle was regular and 30 days, although the duration of menstrual bleeding reduced after the age of 35. When she was 40 years old, her menstrual cycles ranged from 15 to 60 days, and the flow was scanty. She complained of fatigability, listlessness and lack of concentration. No endocrinological examination was performed. She does not have a history of obesity or emaciation. She has never had any episodes of suspected adrenal crisis. The sister of the proband (III-2) was clinically normal and her menarche was at the age of 13 years.

## Intelligence quotient (IQ), mental state and behavioural assessment

Intelligence quotients (IQs) were evaluated using the Wechsler Intelligence Scale for Children-III . Problem behaviours in the children were evaluated by the Child Behaviour Checklist (CBCL).[12] The Beck Depression Inventory (BDI)-II[13] was used to screen depression in the mothers of Probands 1 and 2. The following cut-offs were used for depression: 0–13 points, minimal; 14–19, mild; 20–28, moderate; 29–63, severe. The Structured Clinical Interview for Diagnostic and Statistical Manual of Mental Disorders IV (DSM-IV) Axis Disorders (SCID) was performed on the mother of Proband 1.

## Gonadal histology

Haematoxylin and eosin-stained standard sections from Proband 1 were evaluated. Four-micrometre sections of formalin-fixed, paraffin-embedded tissue specimens were used for immunostaining. Antigen retrieval was performed by boiling in citrate buffer. NR5A1 was used as a primary antibody,[14] and the simple stain MAX-PO system (Nichirei, Tokyo, Japan) was used to detect the primary antibody. For comparison, testes from three foetus obtained at autopsy at the 23th–30th weeks of gestation were examined for NR5A1 expression.

## Mutational analysis

We obtained written informed consent from the patients or parents. The study was approved by the institutional review board. We extracted genomic DNA from peripheral blood. The entire coding regions of *NR5A1* were amplified by PCR (the primer sequences are available on request) and sequenced using Big Dye Dideoxy Sequence Kit (Applied Biosystems, Foster City, CA, USA) and an ABI3130xl automated sequencer (Applied Biosystems). Detected mutations were tested in 60 Japanese healthy controls.

## Three-dimensional (3D) models of NR5A1 proteins

The three-dimensional (3D) models of the ligand-binding domain (LBD) of both wild type (WT) and p.V424-deleted NR5A1 proteins were created using the 3D-JIGSAW web-based interface. Images of the modelled proteins (schematic) were viewed and manipulated using Deep View (The Swiss Institute of Bioinformatics).[15]

## Construction of expression vectors

We generated N-terminal enhanced green fluorescent protein (EGFP)-tagged NR5A1 by cloning the PCR-amplified WT *NR5A1* cDNA in-frame into a pEGFP-C1 (CLONTECH, Palo Alto, CA, USA) via introduced restriction sites (*Eco*R1/*Bam*H1). We created untagged *NR5A1* vectors by removing GFP from the pEGFP-C1-NR5A1 vectors. Three mutants (D257TfsX39, V424del, and L442X) were generated by site-directed mutagenesis (QuikChange IIXL; Stratagene, La Jolla, CA, USA). L442X has a stop codon immediately before the activation function domain 2 (AF2). The luciferase reporter constructs CYP11A1 and CYP19A1 have been described previously.[16,17]

## Cell culture and transfection

We cultured HEK293 cells for luciferase assays and western blots, and COS-7 cells for the GFP study. We transfected WT or mutant plasmids to each cell using Lipofectamine™ 2000 reagent (Invitrogen, Carlsbad, CA, USA) according to the manufacturer's protocol.

## Visualization of subcellular localization

COS-7 cells grown on sterile glass coverslips were transfected with WT or mutant pEGFP-tagged *NR5A1* (0·8 mg). Twenty four hours after transfection, cells were fixed in 2% formaldehyde/PBS. The cover slips were subsequently mounted with Vectashield mounting medium with 4′,6-diamidino-2-phenylindole (DAPI; Vector Laboratories, Burlingame, CA, USA) and were observed under a BX-50 fluorescence microscope (Olympus, Tokyo, Japan).

## Transactivation assay

Untagged-*NR5A1* WT or mutant expression vectors (150 ng/well with CYP11A1 reporter or 30 ng/well with CYP19A1 reporter) were transfected into HEK293 cells with reporters (200 ng/well). The WT and mutant (1:1) were cotransfected with the reporters to determine possible dominant-negative effects. Twenty four hours after transfection, cells were analysed using the Dual Luciferase Reporter assay system (Promega, Madison, WI, USA) according to the manufacturer's protocol. Each result is representative of three independent experiments that yielded similar results. The results are expressed as mean ± standard error of the mean (SEM), and statistical significance was determined by *t*-test.

## Western blotting

We extracted the proteins from whole HEK293 cells, which were transfected with a vector containing either WT or mutant *NR5A1*. Extracted proteins were analysed by SDS-PAGE and Western blotting. We used the primary and secondary antibodies described before.[14]

## Results

### *IQ, mental state and behavioural assessment*

*Family 1.* The proband (II-6) was assessed at 11 years of age. Her full-scale IQ was 114. Her CBCL score was in the borderline clinical range on the 'Withdrawn' domain (Table 1).

The mother of the proband (II-4) scored 40 and 35 (at 38 and 40 years of age) on the BDI–II, indicating severe depression. She was diagnosed with depressive disorder and generalized anxiety disorder by the SCID. She had seven of the nine symptoms in the diagnostic criteria for a major depressive episode. She also mentioned that she had been having excessive anxiety, vague unpleasant emotions and difficulty in controlling her anxiety since childhood.

*Family 2.* The proband (III-5) was assessed with the CBCL at 6 years of age. His scores on the 'Anxious/Depressed' and 'Aggressive Behaviour' domains were in the clinical range. His score on the 'Attention Problems' and 'Rule-Breaking Behaviour' scales were in the borderline clinical range.

*The mother of the proband* (II-3) scored 23 on the BDI-II at 46 years of age, indicating moderate depression.

### *Histopathology*

Samples from Proband 1 obtained at 13 months of age were taken for pathological analysis. Grossly, the gonads were hypoplastic and measured 0·9 × 0·8 cm (on the right) and 1·2 × 0·7 cm (on the left). Histologically, both had similar features (Fig. 1c-1). Müllerian duct-derived tissues were not present. Seminiferous tubules had lost their back-to-back structures and were present in the stroma. The lumen of the seminiferous tubules was primarily composed of Sertoli cells with a minority of spermatogonia as highlighted by nuclear WT1 immunostaining (Fig. 1c-2). Unexpectedly, multiple foci of aggregated foamy probable Leydig cells were noted around the seminiferous tubules. Positive nuclear NR5A1 immunostaining confirmed that these foamy cells were Leydig cells (Fig. 1c-3). From the nuclear accumulation of NR5A1 and the absence of cytoplasmic granular staining patterns, the immunostaining pattern of the NR5A1 protein in the Leydig cells of this patient was found to be similar to that observed in the 3 male foetuses.

### *Mutational analysis*

Mutational analysis of the *NR5A1* gene revealed a heterozygous frameshift mutation, c.768del, D257TfsX39 (Fig. 2) in Proband 1. This mutation was transmitted from her mother and grandmother. This mutation is predicted to alter the protein sequence and create a premature termination codon at codon 296. A heterozygous c.1268_1270delTGG, p.V424del mutation (Fig. 2) was detected in Proband 2. This mutation was transmitted from his mother to Proband 2 and his sister. These two mutations were not observed in the 120 alleles of adult controls.

### *3D models of NR5A1 proteins*

Our model of V424del indicated a change in the loop's shape (Fig. 3, Panels b and c) and the angle of Helix 11 compared with those of WT (Panels d and e). The amino acids in an alpha helix are arranged in a right-handed helical structure in which each amino acid residue corresponds to a 100° turn in the helix and a translation of 0·15 nm along the helical axis. Therefore, the change in the angle of the N-terminal end of Helix 11 was approximately 100°.

### *Visualization of subcellular localization of NR5A1 proteins*

The WT and both mutant proteins were exclusively localized in the nucleus (Fig. 4).

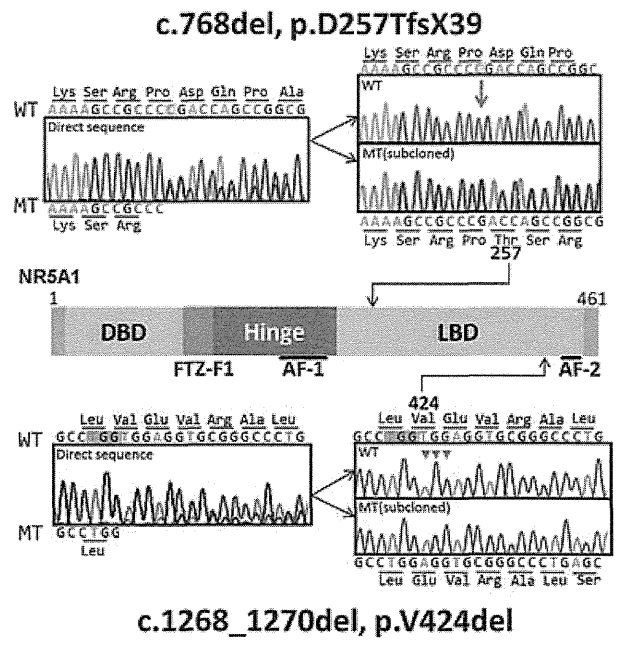


**Fig. 2** Detection of mutations. The functional domains of the NR5A1 protein are shown, including the two mutations described in this study. Representative chromatograms are shown for each mutation. Each mutation was subcloned. The DNA-binding domain (DBD) containing two zinc-finger motifs is indicated. The FtzF1 box stabilizes protein binding to DNA. The hinge region is important for stabilizing the ligand-binding domain (LBD) and interacts with other proteins that control NR5A1 transcriptional activity. The activation function 2 (AF2) domain recruits cofactors necessary for NR5A1 transactivating activity.

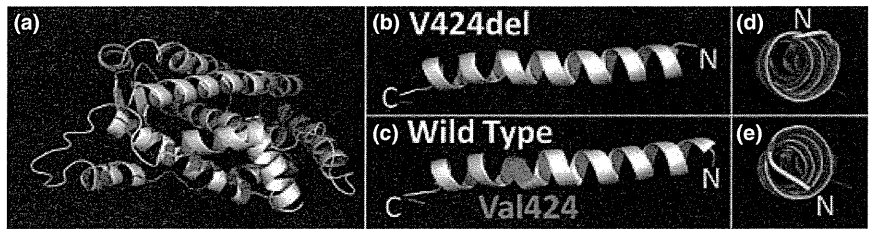


**Fig. 3** 3D models of wild type (WT) and mutated NR5A1 proteins. 3D models of the whole LBD (CYS407-GLY442) (a) and Helices 10 and 11 of the LBD of the WT (b) and V424del-mutated NR5A1 proteins (c) were obtained with the use of the 3D-JIGSAW web-based interface. Val 424 in the WT protein is shown in pink, and the N-terminal side end of Helix 11 is shown in yellow. Note the change of the angle of N-terminal end of Helix 11 (d and e) indicating the shift of the position of the AF2 domain in Helix 12 (red arrow in a).

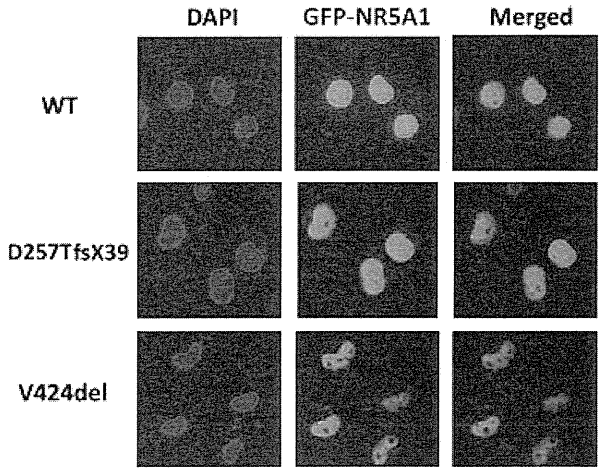


**Fig. 4** Cellular localization of NR5A1 mutants. Cellular localization of GFP-NR5A1 fusion proteins (green) generated and expressed in COS-7 cells with the use of a pEGFP-C1 vector. Wild type (WT) NR5A1 showed nuclear localization. Expression and localization patterns similar to that of the WT are seen for the V424del and the D257fs mutants.

### *Transactivation assay*

The analysis of WT and mutant NR5A1 functions showed impaired activity for the three mutants (D257fs, V424del and L442X) on NR5A1 target gene promoters (Fig. 5). D257fs showed residual transactivation activity of WT NR5A1 (CYP11A1: 60·0 ± 0·12; CYP19A1: 23·9 ± 2·3). V424del markedly impaired activities, which were the same as that observed for the empty vector in both promoters. L442X had the same activity as that observed for the empty vector in both CYP11A1 and CYP19A (data not shown). Cotransfection of the mutants (D257fs or V424del) in a 1:1 ratio with WT *NR5A1* did not impair the transactivation capacity of the WT protein, indicating that no dominant-negative effect occurred.

### *Western blot analysis*

The WT-NR5A1 protein and the V424del protein were detected as the same size bands. The D257fs protein was not detected (data not shown).

## Discussion

We sequenced *NR5A1* in a cohort of 46,XY DSD patients with varying degrees of hypospadia and found 2 unrelated families with a novel heterozygous *NR5A1* mutation. Two 46,XY mutation carriers showed severe submasculinization. Each mutation was transmitted from mothers. Two 46,XX mutation carriers showed premature ovarian insufficiency. Notably, we investigated *NR5A1* mutation carriers' mental status for the first time and found one 46,XX mutation carrier who was depressed and had anxiety disorder and another who was depressed.

We confirmed that two novel *NR5A1* mutations (D257fs and V424del) caused losses of function, without dominant-negative effects, thus resulting in haploinsufficiency. The D257fs (c.768del) mutation, which lacked approximately 85% of the LBD, had some residual activity *in vitro*. D257 is located at exon 4, which is not the last exon, and D257fs has a stop codon that is located downstream of 39 extra amino acids. Thus, the D257fs transcript is likely to be degraded by nonsense-mediated decay, leading to haploinsufficiency *in vivo*. V424del (c.1268_1270del-TGG) was predicted to result in the deletion of an amino acid in the LBD of NR5A1. V424del is highly conserved and is located in Helix 11 of the LBD. The change in the angle of Helix 11 indicated by our 3D model was predicted to dramatically alter NR5A1 activity, consistent with the failure of mutant NR5A1 to transactivate promoters.

Our findings suggested that *NR5A1* mutations resulted in psychiatric symptoms in 46,XX patients. Indeed, among 4 (46,XX) mutation carriers, two showed psychiatric symptoms; anxiety and depression were present in the mother of Proband 1, and there was depression in the mother of Proband 2. The results of the BDI-II indicated that both mothers had moderate to severe depression. The mother of Proband 1 was further diagnosed with major depression and general anxiety disorder by the SCID. Unfortunately, it is uncertain whether the mother of Proband 2 had anxiety, because she refused further mental assessment. The grandmother of Proband 1 and the sister of Proband 2 also declined to undergo any psychological assessment. Some important issues should be discussed regarding psychiatric symptoms. Firstly, we speculate that psychiatric symptoms in 46,XX individuals are due to decreased expression of *NR5A1* target genes in VMH, judging from the phenotypes of VMH-specific *Nr5a1*$^{-/-}$ mice, showing increased anxiety behaviour compared with their

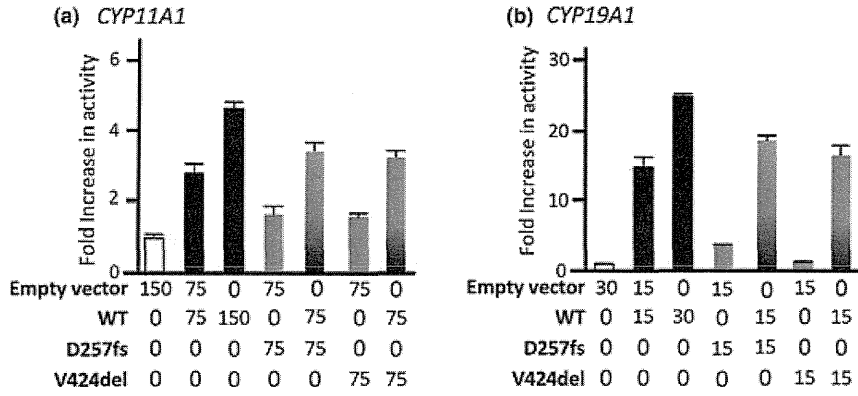


**Fig. 5** Assays of NR5A1 transcriptional activity. The transcriptional activities of wild type (WT) NR5A1 (black bar) and the mutants (blue and red bar) were studied with the use of CYP11A1 (a) and CYP19A1 (b) promoters in HEK293 cells. Results are expressed as fold activity over empty vector (white bar). The under numbers show the concentrations (in ng) of the vectors. D257fs resulted in loss of function (WT: D257fs, CYP11A1, $P < 0{\cdot}05$ and CYP19A, $P < 0{\cdot}002$), no dominant-negative effect (WT1 allele: WT+D257fs, CYP11A1, $P > 0{\cdot}12$ and CYP19A, $P > 0{\cdot}07$) and haploinsufficiency (WT2 alleles: WT+D257fs, CYP11A1, $P < 0{\cdot}02$ and CYP19A, $P < 0{\cdot}001$). V424del showed loss of function (WT: V424del, CYP11A1 $P < 0{\cdot}02$ and CYP19A, $P < 0{\cdot}005$), no dominant-negative effect (WT1 allele: WT+V424del, CYP11A1, $P > 0{\cdot}16$ and CYP19A, $P > 0{\cdot}29$) and haploinsufficiency (WT2 alleles: WT+V424del, CYP11A1, $P < 0{\cdot}01$ and CYP19A $P < 0{\cdot}002$). Data represent the mean of 3 independent experiments, each performed in triplicate. The T-bars represent the standard error of the mean (SEM). Cotransfection of mutants with WT NR5A1 did not show a dominant-negative effect.

WT counterparts.[18] As the knockout mouse mutation is homozygous and all *Nr5a1* regulated functions are lost in VMH, whereas human mutations are heterozygous, psychiatric symptoms in mice might not be seen in all human patients. Possible target genes in the VMH are brain-derived neurotrophic factor (*BDNF*) and corticotrophin-releasing hormone receptor 2 (*CRHR2*), as these genes are related to stress and anxiety.[19] Secondly, psychiatric symptoms have not been reported in any 46, XX mutation carriers in the literature. To our knowledge, more than 20 (46,XX) mutation carriers, including five children have been reported to date.[4,20–28] These patients were probably not evaluated psychiatrically. Alternatively, psychiatric symptoms might become more apparent with age. Third, in 46,XX adult carriers, psychiatric status may be related to having a DSD child and suffering from POI. In our study, the mother of Proband 1 showed separation anxiety during childhood, indicating that some of her psychiatric symptoms must have existed before having a DSD child or suffering from POI. Fourth, in 46,XY mutation adult and child carriers, exploring whether *NR5A1* mutations cause psychiatric symptoms is difficult. Carriers of 46, XY mutations have DSD or azoospermia, which highly affects psychiatric status as observed in patients with other DSDs.[29] We cannot dissect their pathogenesis that is a direct effect of *NR5A1* mutations *vs* the psychiatric effects of adaptation to DSD or azoospermia, although the two probands in our study had some problems in their behaviour as indicated by the CBCL. Moreover, there may be sexual dimorphism in psychiatric symptoms associated with NR5A1, similar to the higher prevalence of depression and anxiety among females in the general population. Fifth, the possibility that these mothers' psychiatric symptoms could simply represent the incidence in the general population and/or simply be the result of family and personal problems cannot be completely ruled out.

The phenotypes of our 46,XY probands (hypospadias without adrenal insufficiency) were consistent with previous reports. In 2009, Kohler *et al.*[30] found three *NR5A1* mutations in 60 patients with hypospadias. In 2011, Allali *et al.* reported one of 33 patients with hypospadias.[28] Taken together, *NR5A1* mutation carriers were found in approximately 5% (6/127) of hypospadias cases.

We confirmed that in females, *NR5A1* heterozygous mutations are associated with premature ovarian insufficiency without adrenal insufficiency. We found four (46,XX) mutation carriers through family analysis, of whom two (the mother and grandmother of Proband 1) had premature ovarian insufficiency. The mother of Proband 2 had seemingly normal ovarian function. The long-term ovarian function of the sister of Proband 2 is not yet clear although her breasts developed normally and her menarche began spontaneously.

We found abundant Leydig cells in the testes of a 13-month-old patient. In previous reports, clusters of Leydig cells were observed in four cases of *NR5A1* mutations in patients aged from 6 months to 2 years,[21,23,26] similar to our observation. Normally, Leydig cells are not recognized after mini-puberty until immediately before puberty. Leydig cells before mini-puberty are called foetal Leydig cells (FLCs), and those after puberty are adult Leydig cells (ALCs).[31,32] We assume that the abundant Leydig cells found in our patient are FLCs because of the age of the patient and the immunostaining pattern; the patient was 13 months old, and ALCs are rarely observed at this age. Recently, Cools *et al.*[33] reported Leydig cell hyperplasia in a pubertal 13-year-old mutation carrier. They showed a homogenous NR5A1 staining pattern in the nuclei and a granular staining pattern in the cytoplasm of ALCs in the carrier and a normal adult, while this pattern was observed in the nuclei of FLCs in a normal foetus. The immunostaining pattern in our

patient was similar to that observed in FLCs. The three possible explanations as to why FLCs remained in our case are as follows: Firstly, *NR5A1* may control target gene (s) that determine the fate of FLCs. Second, cells are more visible because of fat accumulation in the cytoplasm. Indeed, Camats *et al.*[26] reported vacuolization of Leydig cells in 2-year-old patients because of fat accumulation. Third, FLC hyperplasia is possible owing to increased secretion of HCG by the placenta and foetal pituitary LH. Ogata[34] reported that Leydig cells had increased in number and were swollen with abundant lipoid material in the testes at the age of 14 months in a patient with congenital lipoid adrenal hyperplasia. This report supports the second and third hypotheses. The mechanistic details leading to residual FLC accumulation remain to be elucidated.

## Conclusions

We have described two families with novel heterozygous *NR5A1* mutations, D257TfsX39 and V424del. The 46,XY mutation carriers had severe submasculinization. The 46,XX mutation carriers showed primary ovarian insufficiency. Our experience suggests that anxiety and/or depression might be psychiatric symptoms of 46,XX mutation carriers. Psychiatric symptoms in human *NR5A1* mutation carriers should be elucidated, not only in affected members but also in as many other family members as possible.

## Acknowledgements

We are extremely grateful to Prof. Takao Takahashi for the fruitful discussions. We also thank Dr. Toshihiko Yanase for providing the CYP19A1-luc reporter, Dr. Maki Fukami for providing the plasmid containing *NR5A1* cDNA and the CYP11A1-luc reporter, Dr. Kenichiro Morohashi for providing the Ad4BP (NR5A1) antibody and Ms. Fumiko Kato for her technical assistance.

This work was supported in part by a Grant from the Ministry of Health, Labour and Welfare of Japan (grant number: Jitsuyoka (Nanbyo) – Ippan – 014).

## Disclosures

All the authors declare that they are not aware of any potential financial or other conflict of interest related to this work.

## References

1 Luo, X., Ikeda, Y. & Parker, K.L. (1994) A cell-specific nuclear receptor is essential for adrenal and gonadal development and sexual differentiation. *Cell*, **77**, 481–490.

2 Zhao, L., Bakke, M. & Parker, K.L. (2001) Pituitary-specific knockout of steroidogenic factor 1. *Molecular and Cellular Endocrinology*, **185**, 27–32.

3 Jeyasuria, P., Ikeda, Y., Jamin, S.P., *et al.* (2004) Cell-specific knockout of steroidogenic factor 1 reveals its essential roles in gonadal function. *Molecular Endocrinology*, **18**, 1610–1619.

4 Lourenco, D., Brauner, R., Lin, L., *et al.* (2009) Mutations in NR5A1 associated with ovarian insufficiency. *The New England Journal of Medicine*, **360**, 1200–1210.

5 Yokoya, S. (1983) Measurement of Penile and clitoral size in pre-term and term newborns, infants, and children; toward earlier recognition of congenital endocrine disorders. *Clinical Endocrinology*, **31**, 1215–1220.

6 Ito, J., Tanaka, T., Horikawa, R., *et al.* (1993) Clinical study on the time-resolved fluoroimmunoassay of Serum luteinizing hormone and follicle stimulating hormone in children: The change of serum gonadotropins in LHRH test and night time secretion during puberty. *Journal of Japan Pediatric Society*, **97**, 1789–1796.

7 Winter, J.S., Taraska, S. & Faiman, C. (1972) The hormonal response to HCG stimulation in male children and adolescents. *The Journal of Clinical Endocrinology and Metabolism*, **34**, 348–353.

8 Sakakura, K. & Kohhka, K. (2005) Menopause woman's reference range of hypophysis and sex hormone using automatic electrochemiluminescence immunoassay analyzer "Modular Analytics". *Clinical Endocrinology*, **53**, 545–551.

9 Anasti, J. (1998) Premature ovarian failure: an update. *Fertility and Sterility*, **70**, 1–15.

10 Fujieda, K. & Matsuura, N. (1987) Growth and maturation in the male genitalia from birth to adolescence. I. Change of testicular volume. *Acta Paediatrica Japonica*, **29**, 214–219.

11 Matsuo, N., Anzo, M., Sato, S., *et al.* (2000) Testicular volume in Japanese boys up to the age of 15 years. *European Journal of Pediatrics*, **159**, 843–845.

12 Achenbach, T.M. & Rescorla, L.A., ed. (2001) Manual for the ASEBA School-Age Forms and Profiles. University of Vermont, Research Center for Children, Youth, and Families, Burlington, VT.

13 Beck, A.T., Ward, C.H., Mendelson, M., *et al.* (1961) An inventory for measuring depression. *Archives of General Psychiatry*, **4**, 561–571.

14 Yokoyama, C., Komatsu, T., Ogawa, H., *et al.* (2009) Generation of rat monoclonal antibodies specific for Ad4BP/SF-1. *Hybridoma (Larchmt)*, **28**, 113–119.

15 Bates, P.A., Kelly, L.A. & MacCallum, R.M., *et al.* ( 2001) Enhancement of protein modeling by human intervention in applying the automatic programs 3D-JIGSAW and 3D-PSSM. *Proteins*, **45**, 39–46.

16 Hasegawa, T. (2004) Testicular dysgenesis without adrenal insufficiency in a 46,XY patient with a heterozygous inactive mutation of steroidogenic factor-1. *The Journal of Clinical Endocrinology and Metabolism*, **89**, 5930–5935.

17 Oba, K., Yanase, T., Nomura, M., *et al.* (1996) Structural characterization of human Ad4bp (SF-1) gene. *Biochemical and Biophysical Research Communications*, **226**, 261–267.

18 Zhao, L., Kim, K.W., Ikeda, Y., *et al.* (2008) Central nervous system-specific knockout of steroidogenic factor 1 results in increased anxiety-like behavior. *Molecular Endocrinology*, **22**, 1403–1415.

19 Kim, K.W., Zhao, L. & Parker, K.L. (2009) Central nervous system-specific knockout of steroidogenic factor 1. *Molecular and Cellular Endocrinology*, **300**, 132–136.

20 Achermann, J.C., Ozisik, G., Ito, M., *et al.* (2002) Gonadal determination and adrenal development are regulated by the orphan nuclear receptor steroidogenic factor-1, in a dose-dependent manner. *The Journal of Clinical Endocrinology and Metabolism*, **87**, 1829–1833.

21 Coutant, R., Mallet, D., Lahlou, N., *et al.* (2007) Heterozygous mutation of steroidogenic factor-1 in 46,XY subjects may mimic partial androgen insensitivity syndrome. *The Journal of Clinical Endocrinology Metabolism*, **92**, 2868–2873.
22 Philibert, P., Zenaty, D., Lin, L., *et al.* (2007) Mutational analysis of steroidogenic factor 1 (NR5a1) in 24 boys with bilateral anorchia: a French collaborative study. *Human Reproduction*, **22**, 3255–3261.
23 Warman, D.M., Costanzo, M. & Marino, R., *et al.* (2011) Three new SF-1 (NR5A1) gene mutations in two unrelated families with multiple affected members: within-family variability in 46, XY subjects and low ovarian reserve in fertile 46,XX subjects. *Hormone Research in Paediatrics*, **75**, 70–77.
24 Janse, F., de With, L.M., Duran, K.J., *et al.* (2012) Limited contribution of NR5A1 (SF-1) mutations in women with primary ovarian insufficiency (POI). *Fertility and Sterility*, **97**, 141–146.e142.
25 Kohler, B., Lin, L., Ferraz-de-Souza, B., *et al.* (2008) Five novel mutations in steroidogenic factor 1 (SF1, NR5A1) in 46,XY patients with severe underandrogenization but without adrenal insufficiency. *Human Mutation*, **29**, 59–64.
26 Camats, N.P.A., Fernández-Cancio, M., Andaluz, P., *et al.* (2012) Ten novel mutations in the NR5A1 gene cause disordered sex development in 46,XY and ovarian insufficiency in 46,XX individuals. *The Journal of Clinical Endocrinology and Metabolism*, **97**, E1294–E1306.
27 Lin, L., Philibert, P., Ferraz-de-Souza, B., *et al.* (2007) Heterozygous missense mutations in steroidogenic factor 1 (SF1/Ad4BP, NR5A1) are associated with 46,XY disorders of sex development with normal adrenal function. *The Journal of Clinical Endocrinology and Metabolism*, **92**, 991–999.
28 Allali, S., Muller, J.B., Brauner, R., *et al.* (2011) Mutation analysis of NR5A1 encoding steroidogenic factor 1 in 77 patients with 46, XY disorders of sex development (DSD) including hypospadias. *PLoS ONE*, **6**, e24117.
29 Johannsen, T.H., Ripa, C.P., Mortensen, E.L., *et al.* (2006) Quality of life in 70 women with disorders of sex development. *European Journal of Endocrinology*, **155**, 877–885.
30 Kohler, B., Lin, L., Mazen, I., *et al.* (2009) The spectrum of phenotypes associated with mutations in steroidogenic factor 1 (SF-1, NR5A1, Ad4BP) includes severe penoscrotal hypospadias in 46,XY males without adrenal insufficiency. *European Journal of Endocrinology*, **161**, 237–242.
31 Codesal, J., Regadera, J., Nistal, M., *et al.* (1990) Involution of human fetal Leydig cells. An immunohistochemical, ultrastructural and quantitative study. *Journal of Anatomy*, **172**, 103–114.
32 Prince, F.P. (1984) Ultrastructure of immature Leydig cells in the human prepubertal testis. *The Anatomical Record*, **209**, 165–176.
33 Cools, M., Hoebeke, P., Wolffenbuttel, K.P., *et al.* (2012) Pubertal androgenization and gonadal histology in two 46,XY adolescents with NR5A1 mutations and predominantly female phenotype at birth. *European Journal of Endocrinology*, **166**, 341–349.
34 Ogata, T., Matsuo, N., Saito, M., *et al.* (1989) The testicular lesion and sexual differentiation in congenital lipoid adrenal hyperplasia. *Helvetica Paediatrica Acta*, **43**, 531–538.
35 Ogata, T., Matsuo, N., Saito, M., *et al.* (1989) The testicular lesion and sexual differentiation in congenital lipoid adrenal hyperplasia. *Helvetica Paediatrica Acta* **43**, 531–538.

PLOS ONE

# Quantitative and Sensitive Detection of *GNAS* Mutations Causing McCune-Albright Syndrome with Next Generation Sequencing

**Satoshi Narumi[1☯]*, Kumihiro Matsuo[2☯], Tomohiro Ishii[1], Yusuke Tanahashi[2], Tomonobu Hasegawa[1]**

**1** Department of Pediatrics, Keio University School of Medicine, Tokyo, Japan, **2** Department of Pediatrics, Asahikawa Medical University, Hokkaido, Japan

## Abstract

Somatic activating *GNAS* mutations cause McCune-Albright syndrome (MAS). Owing to low mutation abundance, mutant-specific enrichment procedures, such as the peptide nucleic acid (PNA) method, are required to detect mutations in peripheral blood. Next generation sequencing (NGS) can analyze millions of PCR amplicons independently, thus it is expected to detect low-abundance *GNAS* mutations quantitatively. In the present study, we aimed to develop an NGS-based method to detect low-abundance somatic *GNAS* mutations. PCR amplicons encompassing exons 8 and 9 of *GNAS*, in which most activating mutations occur, were sequenced on the MiSeq instrument. As expected, our NGS-based method could sequence the *GNAS* locus with very high read depth (approximately 100,000) and low error rate. A serial dilution study with use of cloned mutant and wildtype DNA samples showed a linear correlation between dilution and measured mutation abundance, indicating the reliability of quantification of the mutation. Using the serially diluted samples, the detection limits of three mutation detection methods (the PNA method, NGS, and combinatory use of PNA and NGS [PNA-NGS]) were determined. The lowest detectable mutation abundance was 1% for the PNA method, 0.03% for NGS and 0.01% for PNA-NGS. Finally, we analyzed 16 MAS patient-derived leukocytic DNA samples with the three methods, and compared the mutation detection rate of them. Mutation detection rate of the PNA method, NGS and PNA-NGS in 16 patient-derived peripheral blood samples were 56%, 63% and 75%, respectively. In conclusion, NGS can detect somatic activating *GNAS* mutations quantitatively and sensitively from peripheral blood samples. At present, the PNA-NGS method is likely the most sensitive method to detect low-abundance *GNAS* mutation.

**Citation:** Narumi S, Matsuo K, Ishii T, Tanahashi Y, Hasegawa T (2013) Quantitative and Sensitive Detection of *GNAS* Mutations Causing McCune-Albright Syndrome with Next Generation Sequencing. PLoS ONE 8(3): e60525. doi:10.1371/journal.pone.0060525

**Editor:** Joseph Devaney, Children's National Medical Center, United States of America

**Received** October 2, 2012; **Accepted** February 28, 2013; **Published** March 25, 2013



**Funding:** This work was supported by the Grant-in-Aid for Young Scientists (B) (24791087) from the Japan Society for the Promotion of Science, and the Health Science Research Grant for Research on Applying Health Technology [Jitsuyoka (Nanbyo)-Ippan-014] from the Ministry of Health, Labour and Welfare, Japan. The funders had no role in study design, data collection and analysis, decision to publish, or preparation of the manuscript.

**Competing Interests:** The authors have declared that no competing interests exist.

* E-mail: sat_naru@hotmail.com

☯ These authors contributed equally to this work.

## Introduction

The rapid emergence of next generation sequencing (NGS) is revolutionizing medical sciences. NGS now allows clinical investigators to analyze transcriptome, exome and genome from small amounts of DNA/RNA. NGS is also available for ultra-deep sequencing of PCR amplicons, microRNA and microbiomes. NGS-based approaches have brought remarkable advances in a broad range of medical research areas, such as studies of rare Mendelian disorders [1] and surveillance of infectious disease outbreaks [2]. NGS has also provided a wealth of new information for cancer genomics, owing in part to the ultra-deep amplicon sequencing of cancerous and precancerous cells [3]. Because NGS can analyze millions of DNA fragments simultaneously and independently, low abundance mutations of oncogenes have now become readily detectable. However, in contrast to advances in understanding of somatic mutations associated with cancer, knowledge about somatic mutations causing benign congenital disorders remains very limited.

McCune-Albright syndrome (MAS; OMIM #174800) is a rare congenital disorder hallmarked by osseous fibrous dysplasia, café-au-lait skin pigmentation and various endocrine hyperfunction, *e.g.*, peripheral precocious puberty, Cushing syndrome and functional pituitary adenoma [4,5]. MAS is caused by activating mutations of *GNAS*, encoding the stimulatory G-protein alpha subunit [6]. Mutations are exclusively present in the somatic mosaic state, probably because the nonmosaic state leads to early embryonic lethality. Clinical manifestations of MAS are highly variable in all three lesions, presumably due to variability of mutation abundance among affected tissues.

In MAS patients, mutation abundance is generally low in unaffected tissues. Thus, mutations in peripheral blood leukocytes (PBL) cannot be detected by standard PCR-based Sanger sequencing, while mutations in affected lesions (*e.g.*, surgical bone specimens) can. Based on the fact that the vast majority of activating *GNAS* mutations occurs in the Arg201 residue, Candeliere *et al.* developed the method for selective enrichment of Arg201 *GNAS* mutations using a series of nested PCR and restriction enzyme digestion [7]. Subsequently, the second enrichment method with use of a peptide nucleic acid (PNA) probe, which forms hybrids with wildtype DNA and inhibits PCR

amplification, was developed [8]. Mutation detection rate from PBL samples with these two methods are typically around 50% [9–11]. Of interest, mutation detection rate increases up to 90% when DNA sample derived from the affected lesion is available [10]. This implies that diagnostic performance of the two methods is still inadequate.

In the present study, we developed a novel NGS-based method that can detect low-abundance *GNAS* mutations quantitatively and sensitively. We compared diagnostic performance of the NGS-based method with that of the PNA method, by a serial dilution study and a mutation detection study using 16 MAS patient-derived PBL samples.

## Materials and Methods

### PCR with or without the PNA probe

The overview of mutation detection methods is shown in **Figure 1**. All DNA samples used in the study was extracted from PBL with the Gentra Puregene Blood Kit (Qiagen, Hilden, Germany). Partial region of the *GNAS* locus (chr20:57484398-57484647; hg19), in which nucleotides 598 to 711 (begins at the first ATG codon) were included, was PCR-amplified with or without the PNA probe. The PCR mixture (final volume 20 μL) contained 100 ng genomic DNA, 0.25 mM dNTPs, primers (0.25 μM each), and 1 U Herculase II Fusion DNA Polymerases in reaction buffer (Agilent Technologies, Santa Clara, CA), with or without 30 μM PNA probe (Panagene Inc., Daejeon, Korea). The PCR conditions were as follows: initial denaturation at 98°C for 30 s; 35 cycles at 98°C for 10 s (denaturation), 68°C for 60 s (hybridization), 55°C for 30 s (annealing) and 72°C for 30 s (extension) with a final extension at 72°C for 5 min. The sequences of the PNA and primers were as follows: PNA Gly-$NH_2$-CGC TGC CGT GTC-HAc; sense primer 5′-CTA CAC GAC GCT CTT CCG ATC TGT TTC AGG ACC TGC TTC GC-3′; and antisense primer 5′-GTG ACT GGA GTT CAG ACG TGT GCT CTT CCG ATC TCA CAG CAT CCT ACC GTT GAA-3′ (adaptor sequences used in Illumina platform are underlined). Generated PCR products were purified with the Agencourt AMPure XP Bead system (Beckman Coulter Genomics, Essex, UK), and were subject to both Sanger sequencing and NGS.

### Mutation detection by Sanger sequencing and NGS

For Sanger sequencing, we used the BigDye Dideoxy Sequence Kit (Life Technologies, Carlsbad, CA) and the ABI3130*xl* sequencer (Life Technologies). Presence/absence of mutations was judged based on visual inspection of each sequence chromatogram.

As for NGS, we performed 15 cycles of second PCR using diluted first PCR products to add the attachment sites (P5 and P7) and the index sequence, which are used in Illumina multiplexed sequencing. The PCR mixture (final volume 20 μL) contained 1 μL purified first PCR product (diluted 1:20 with pure water), 0.25 mM dNTPs, primers (0.25 μM each), and 1 U Herculase II Fusion DNA Polymerases in reaction buffer. The PCR conditions were as follows: initial denaturation at 98°C for 30 s; 15 cycles at 98°C for 10 s, 55°C for 20 s and 72°C for 30 s with a final extension at 72°C for 5 min. The sequences of the primers were as follows: sense primer: 5'- AAT GAT ACG GCG ACC ACC GAG ATC TAC ACT CTT TCC CTA CAC GAC GCT CTT CCG ATC T-3'; and antisense primer: 5'- CAA GCA GAA GAC GGC ATA CGA GAT NNN NNN GTG ACT GGA GTT CAG ACG TGT-3' (P7 and P5 attachment sites are underlined. NNN NNN in the antisense primer denotes index-specific sequence). The second PCR products were purified with the AMPure system, and were quantified with the Qubit dsDNA HS Assay Kit (Life Technologies). In each NGS run, 16 samples were multiplexed per pool. To improve base call accuracy, an equimolar quantity of the PhiX control (Illumina, San Diego, CA) was added to the pool.

Pooled samples were pair-end sequenced on the MiSeq instrument with at least 30 cycles and an index read. Base calling, read filtering and demultiplexing were performed according to the standard Illumina processing pipeline. Sequence reads were mapped to the *GNAS* genomic sequence with Bowtie [12]. We used SAMtools to calculate read depth and nucleotide frequencies for each position of the amplicons [13]. Filtering threshold was set to Q35, which is equivalent to the probability of an incorrect base call 1 in 3160 times. For each experiment, three control PBL DNA samples were analyzed to define the experiment-specific reference upper limit of the variant call (z-score equal or more than 2.5 were defined as positive). All DNA samples were amplified and sequenced twice.

### Serial dilution of cloned mutant DNAs

A first PCR product generated from an R201H mutation carrying patient was cloned into the pCR2.1-TOPO vector (Life Technologies). We prepared wildtype or mutant DNA (each 1 ng/ μL) by diluting sequence-verified plasmids. Then, we diluted cloned mutant DNA into cloned wildtype DNA to 1/10 [relative mutation abundance (RMA), 10%], 1/100 (1%), 1/333 (0.3%), 1/1,000 (0.1%), 1/3,333 (0.03%) and 1/10,000 (0.01%). Serially diluted DNA samples were subject to sequence analyses described above.

### Clinical samples

In a comparative mutation detection study, 16 PBL genome samples derived from MAS patients (6 boys and 10 girls) were used. The 16 patients had classic form of MAS with two or three features of the triad (osseous fibrous dysplasia, café-au-lait skin pigmentation and endocrine hyperfunction) (**Table 1**). Fibrous dysplasia, café-au-lait skin pigmentation and endocrine hyperfunction were observed in 14 (88%), 12 (75%) and 14 (88%), respectively. Eight subjects (50%) had all three features. Observed endocrine dysfunction includes peripheral precocious puberty (N = 9), functional thyroid adenoma (N = 3), functional pituitary adenoma (N = 2) and Cushing syndrome (N = 2) (**Table 1**).

### Ethics statement

The study was approved by the Institutional Review Boards of Asahikawa Medical University and Keio University School of Medicine. Written informed consent for molecular studies was obtained from the subjects or his/her parents.

## Results

### GNAS amplicon sequencing by NGS

We designed chimeric primer pairs, containing both locus-specific and adapter sequences, to generate PCR amplicons that are directly sequenced on the Illumina MiSeq platform. The amplicon covers two known sites of activating *GNAS* mutations (*i.e.*, Arg201 and Gln227 [14]), thus would be expected to detect most mutations causing MAS. This experimental design allowed us to generate very high read depth per sample (approximately 100,000) with low error rate (mean±SD, 0.011±0.005%) (data not shown).

### Quantitative detection of a GNAS mutation

To test the ability of the NGS-based mutation detection to provide quantitative data, we conducted a serial dilution study

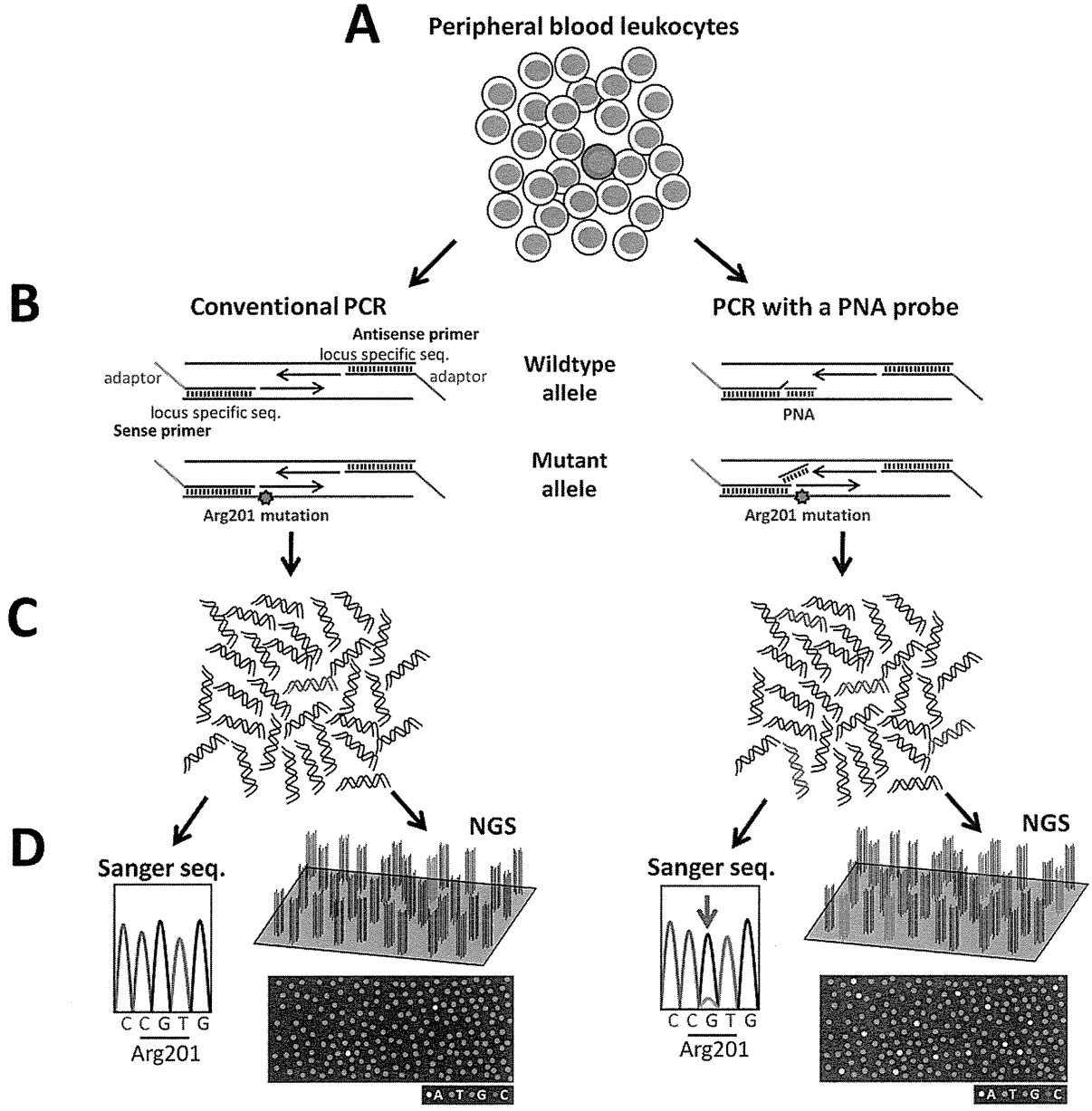


**Figure 1. Schematic diagramas showing an overview of mutation detection methods.** (**A**) In patients with McCune-Albright syndrome, the proportion of mutation-carrying cells (colored red) is low in peripheral blood leukocytes (PBL). (**B**) In the present study, PCR amplification was conducted in the absence (*left panel*) or presence (*right panel*) of the peptide nucleic acid (PNA) probe. The PNA probe preferentially hybridizes to wildtype PCR fragments (colored black) and inhibits their amplification. This results in enrichment of mutant PCR fragments (colored red). We used chimeric PCR primers, containing both locus-specific and adapter sequences, to generate amplicons that are sequenced on the Illumina platform. (**C**) PCR without the PNA probe produces PCR amplicons, of which relative proportion between wildtype (colored black) and mutant (colored red) is similar to PBL (*left panel*). In contrast, PNA treatment enriches mutant amplicons (*right panel*). (**D**), PCR amplicons were analyzed by both Sanger sequencing and next generation sequencing ('NGS'). Due to low mutation abundance, mutations cannot be detected in amplicons generated without the PNA probe (*left panel*), while they can be detected in PNA-treated amplicons (*right panel,* an arrow indicates the mutation). In the MiSeq platform, clonal clusters, each derived from a single DNA molecule, are generated on a flow cell, and are sequenced base-by-base simultaneously and independently. The diagrams under the schematic flow cells show imaginative optically scanned data of the cycle corresponding to the mutated nucleotide. In a sample without PNA treatment, the mutant amplicons can be recognized on the flow cell (*left panel*). Mutant-enriched samples are also analyzable by NGS (*right panel*).
doi:10.1371/journal.pone.0060525.g001

using cloned plasmid DNA samples (wildtype or R201H). We serially diluted mutant DNA into wildtype DNA, and measured mutant abundance with NGS. As we expected, a linear correlation between true mutant abundance and measured relative mutation abundance (NGS-measured RMA; defined as the proportion of sequence reads containing the mutation), was observed down to 0.01% (**Figure 2**), indicating reliable quantification.

**Table 1.** Characteristics of the study subjects.

| ID | Sex | MAS features | | | Relative mutation abundance (%) | Mutation detection method | | |
|---|---|---|---|---|---|---|---|---|
| | | FD | Skin lesion | Endocrine hyperfunction | | PNA | NGS | PNA-NGS |
| 1 | F | Present | Present | Peripheral PP | 12.4 | R201C | R201C | R201C |
| 2 | M | Present | Present | Functional pituitary adenoma*, Functional thyroid adenoma | 4.2 | R201C | R201C | R201C |
| 3 | M | Present | Absent | Cushing syndrome | 3.4 | R201H | R201H | R201H |
| 4 | F | Absent | Present | Peripheral PP | 2.9 | N.D. | R201C | R201C |
| 5 | F | Present | Present | Peripheral PP | 1.4 | R201H | R201H | R201H |
| 6 | M | Present | Present | Absent | 0.81 | R201H | R201H | R201H |
| 7 | M | Present | Present | Cushing syndrome | 0.67 | R201H | R201H | R201H |
| 8 | F | Present | Present | Peripheral PP, Functional thyroid adenoma | 0.55 | R201H | R201H | R201H |
| 9 | M | Present | Present | Functional thyroid adenoma | 0.28 | R201H | R201H | R201H |
| 10 | M | Present | Absent | Pituitary adenoma** | 0.26 | R201C | R201C | R201C |
| 11 | F | Present | Present | Peripheral PP | <0.03 | N.D. | N.D. | R201C |
| 12 | F | Present | Present | Peripheral PP | <0.03 | N.D. | N.D. | R201H |
| 13 | F | Absent | Present | Peripheral PP, Functional thyroid adenoma | <0.03 | N.D. | N.D. | N.D. |
| 14 | F | Present | Absent | Peripheral PP | <0.03 | N.D. | N.D. | N.D. |
| 15 | F | Present | Absent | Peripheral PP | <0.03 | N.D. | N.D. | N.D. |
| 16 | F | Present | Present | Absent | <0.03 | N.D. | N.D. | N.D. |

Abbreviations: FD, osseous fibrous dysplasia; MAS, McCune-Albright syndrome; N.D., not detected; NGS, next generation sequencing; PNA, the peptide nucleic acid method; PNA-NGS, combinatory use of PNA and NGS; PP, precocious puberty.
*Hyperprolactinemia and GH-producing adenoma.
**GH-producing adenoma.
doi:10.1371/journal.pone.0060525.t001

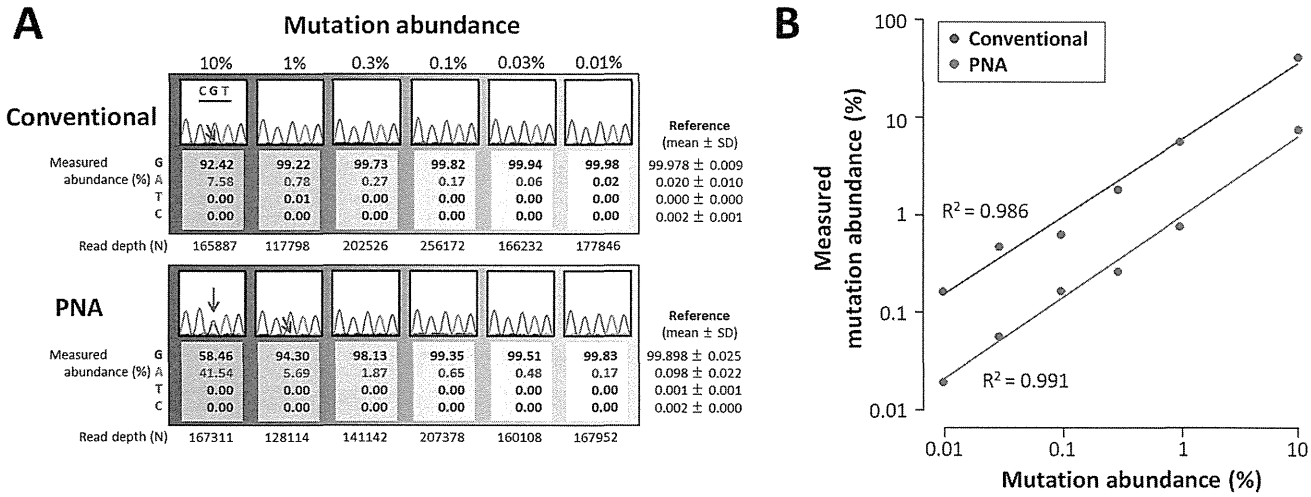


**Figure 2. Results of the serial dilution study.** (**A**) Cloned mutant DNA (R201H mutation) was diluted into cloned wildtype DNA to 1/10 (10%), 1/100 (1%), 1/333 (0.3%), 1/1,000 (0.1%), 1/3,333 (0.03%) and 1/10,000 (0.01%). Serially diluted DNA samples were PCR-amplified with or without the peptide nucleic acid (PNA) probe ('PNA' and 'Conventional'. Each PCR product was analyzed by Sanger sequencing and next generation sequencing (NGS). Partial chromatograms encompassing the GNAS codon 201 (indicated by CGT) are shown. Relative abundance of the c.602 nucleotide (G, A, T and C) measured by NGS is aligned with each chromatogram. The G allele is wildtype, while the A allele is the R201H mutant. Values with a positive test result (defined by z-score of measured mutant abundance; see Materials and Methods for details) are colored red. Experiment-specific reference ranges are also shown. In the 12 chromatograms, the mutant signal could be detected in two PNA-treated samples and one non-treated sample (indicated by red arrows). Contrastingly, the mutation could be detected down to 0.03% by NGS alone, and down to 0.01% by combinatory use of PNA and NGS. (**B**) A serial dilution plot showing a linear correlation between true mutation abundance and measured mutation abundance. Note that both axes are logarithmic. Comparison of mutation abundance values of PNA-treated and untreated samples revealed that the fold enrichment by PNA is about 7, and it was independent of initial abundance.
doi:10.1371/journal.pone.0060525.g002

### Mutation abundance in PBL of MAS patients

To define the distribution of NGS-measured RMA in PBL among MAS patients, we analyzed 16 patient-derived PBL samples. Ten out of 16 genomes had a *GNAS* mutation (R201H, N = 6; R201C, N = 4) of which NGS-measured RMA was more than 0.03% (**Table 1**). NGS-measured RMA ranged from 0.3% to 12.4% (median, 1.1%), which was consistent with the fact that we could not detect those mutations by conventional Sanger sequencing without the PNA probe (data not shown). It is also consistent with the previous genetic knowledge that conventional Sanger sequencing cannot detect *GNAS* mutations in most MAS patient-derived PBL samples [7]. The distributions of NGS-measured RMA were similar between eight patients having all three MAS features and the remaining eight with two features (P = 0.5, Wilcoxon rank sum test).

### Comparison of mutation detection methods

Finally, we compared the diagnostic performance of three mutation detection methods: the PNA method, NGS, and combinatory use of PNA and NGS (PNA-NGS). We assessed the detection limits using the serially diluted samples, and found that NGS could detect the mutation down to 0.03%, while the PNA method alone could detect down to 1% (**Figure 2**). The PNA-NGS method had the lowest detection limit, which was 0.01% (**Figure 2**). We also performed a comparative mutation detection study using the 16 patient-derived PBL genome samples. The PNA method identified mutations in nine out of 16 patients (**Table 1**). All of these mutations were also detected by NGS and PNA-NGS. Among seven patients with a negative result by the PNA method, NGS detected one mutation carrier, and PNA-NGS revealed further two mutation carriers (**Table 1**). Collectively, mutation detection rate of PNA, NGS and PNA-NGS was 56%, 63% and 75%, respectively.

## Discussion

Detecting low-abundance somatic mutations with next generation amplicon sequencing is becoming a robust analytic tool in cancer genomics. In the present study, we demonstrate that this approach is also effective in diagnosis of a benign disorder due to low-abundance somatic mutations, as shown in megalencephaly syndromes very recently [15].

The quantitative nature of NGS allowed us to investigate the distribution of RMA in patient-derived PBL samples. We showed for the first time that NGS-measured RMA in PBL is strikingly variable among MAS patients. NGS-measured RMA in PBL does not correlate with disease severity, as defined by the number of clinical features, indicating that RMA in PBL and affected lesions are not correlated. Similar results have been observed in syndromes due to activation of AKT signaling (Proteus syndrome [16], and megalencephaly syndromes [15]), thus would be a universal feature of congenital syndromes due to somatic activating mutations.

We verified the diagnostic performance of three mutation detection methods (PNA, NGS and PNA-NGS) using a serial dilution study and a comparative mutation detection study. In both studies, the PNA-NGS method was seemed to be most sensitive. Combination of NGS and PNA resulted in 100-fold decrease in assay detection limit as compared with the PNA method alone. Clearly, this improvement will contribute to more accurate molecular diagnosis of MAS.

In the present study, 56% of MAS patients were positive for a *GNAS* mutation by the PNA method. Similar mutation detection rate with the nested PCR method or the PNA method have been reported [9–11]. Of clinical importance, we could detect *GNAS* mutations by the PNA-NGS method in three out of seven 'PNA-negative' MAS patients. This would be not only due to ultra-deep sequencing of NGS, but also due to nature of the mutation detection methods (qualitative *vs* quantitative), because a patient with relatively high RMA (Patient 4 in **Table 1**) was missed by PNA. Considering that mutation detection rate is more than 90% when affected tissue was available [10], we believe that improvement of mutation detection by the PNA-NGS approach is due to increase of true positives, although we cannot discriminate true positives from false positives in the present study. Future studies using paired PBL-affected tissue(s) samples, which have discordant test results (*e.g.*, negative in PBL but positive in affected tissue(s)) will clarify the true diagnostic performance of the PNA-NGS approach.

In summary, we successfully developed an NGS-based mutation detection method for MAS, allowing quantitative and sensitive molecular diagnosis. The PNA-NGS method achieved 100-fold decrease in assay detection limit, as compared with the PNA method. Our study exemplifies the utility of NGS-based approaches to diagnose congenital disorders due to low-abundance somatic mutations from peripheral blood.

## Acknowledgments

We would like to thank the following physicians for sent us clinical samples of MAS patients: Hamajima T (Aichi Children's Health and Medical Center), Hori N (Sanokousei General Hospital), Kamasaki H (Sapporo Medical University School of Medicine), Kamimaki T (Shizuoka City Shimizu Hospital), Kawada Y (Kyushu Rousai Hospital), Motomura K (Nagasaki University), Mukai T (Asahikawa-Kosei General Hospital), Naiki Y (National Center for Child Health and Development), Okada S (Hiroshima University Graduate School of Biomedical Sciences), Suwa T (Gifu University), Tajima T (Hokkaido University School of Medicine), and Tokuhiro E (Odawara Municipal Hospital). We also thank Prof. Takao Takahashi for fruitful discussion.

## Author Contributions

Conceived and designed the experiments: SN TH. Performed the experiments: SN KM. Analyzed the data: SN. Contributed reagents/materials/analysis tools: KM TI YT TH. Wrote the paper: SN.

## References

1. Ng SB, Turner EH, Robertson PD, Flygare SD, Bigham AW, et al. (2009) Targeted capture and massively parallel sequencing of 12 human exomes. Nature 461: 272–276.
2. Mellmann A, Harmsen D, Cummings CA, Zentz EB, Leopold SR, et al. (2011) Prospective genomic characterization of the German enterohemorrhagic Escherichia coli O104:H4 outbreak by rapid next generation sequencing technology. PLoS One 6: e22751.
3. Thomas RK, Nickerson E, Simons JF, Janne PA, Tengs T, et al. (2006) Sensitive mutation detection in heterogeneous cancer specimens by massively parallel picoliter reactor sequencing. Nat Med 12: 852–855.
4. McCune DJ (1936) Osteitis fibrosa cystica; the case of a nine year old girl who also exhibits precocious puberty, multiple pigmentation of the skin and hyperthyroidism. Am J Dis Child 52: 743–744.
5. Albright F, Butler AM, Hampton AO, Smith P (1937) Syndrome characterized by osteitis fibrosa disseminata, areas of pigmentation and endocrine dysfunction, with precocious puberty in females: report of five cases. N Engl J Med 216: 727–746.
6. Weinstein LS, Shenker A, Gejman PV, Merino MJ, Friedman E, et al. (1991) Activating mutations of the stimulatory G protein in the McCune-Albright syndrome. N Engl J Med 325: 1688–1695.

7. Candeliere GA, Roughley PJ, Glorieux FH (1997) Polymerase chain reaction-based technique for the selective enrichment and analysis of mosaic arg201 mutations in G alpha s from patients with fibrous dysplasia of bone. Bone 21: 201–206.
8. Bianco P, Riminucci M, Majolagbe A, Kuznetsov SA, Collins MT, et al. (2000) Mutations of the GNAS1 gene, stromal cell dysfunction, and osteomalacic changes in non-McCune-Albright fibrous dysplasia of bone. J Bone Miner Res 15: 120–128.
9. Hannon TS, Noonan K, Steinmetz R, Eugster EA, Levine MA, et al. (2003) Is McCune-Albright syndrome overlooked in subjects with fibrous dysplasia of bone? J Pediatr 142: 532–538.
10. Lumbroso S, Paris F, Sultan C, European Collaborative S (2004) Activating Gsalpha mutations: analysis of 113 patients with signs of McCune-Albright syndrome--a European Collaborative Study. J Clin Endocrinol Metab 89: 2107–2113.
11. Kalfa N, Philibert P, Audran F, Ecochard A, Hannon T, et al. (2006) Searching for somatic mutations in McCune-Albright syndrome: a comparative study of the peptidic nucleic acid versus the nested PCR method based on 148 DNA samples. Eur J Endocrinol 155: 839–843.
12. Langmead B, Trapnell C, Pop M, Salzberg SL (2009) Ultrafast and memory-efficient alignment of short DNA sequences to the human genome. Genome Biol 10: R25.
13. Li H, Handsaker B, Wysoker A, Fennell T, Ruan J, et al. (2009) The Sequence Alignment/Map format and SAMtools. Bioinformatics 25: 2078–2079.
14. Lee SE, Lee EH, Park H, Sung JY, Lee HW, et al. (2012) The diagnostic utility of the GNAS mutation in patients with fibrous dysplasia: meta-analysis of 168 sporadic cases. Hum Pathol 43: 1234–1242.
15. Riviere JB, Mirzaa GM, O'Roak BJ, Beddaoui M, Alcantara D, et al. (2012) De novo germline and postzygotic mutations in AKT3, PIK3R2 and PIK3CA cause a spectrum of related megalencephaly syndromes. Nat Genet 44: 934–940.
16. Lindhurst MJ, Sapp JC, Teer JK, Johnston JJ, Finn EM, et al. (2011) A mosaic activating mutation in AKT1 associated with the Proteus syndrome. N Engl J Med 365: 611–619.

Atsuko Yoshizawa-Ogasawara*, Sayaka Ogikubo, Mari Satoh, Satoshi Narumi and Tomonobu Hasegawa

# Congenital hypothyroidism caused by a novel mutation of the dual oxidase 2 *(DUOX2)* gene

**Abstract:** The dual oxidase 2 *(DUOX2)* mutation results in an impairment of the hydrogen peroxidase-generating system and is identified as a dyshormonogenic cause of congenital hypothyroidism (CH). Here, we describe two unrelated Japanese girls with CH due to a novel *DUOX2* mutation. They had high serum thyrotropin levels and low free thyroxine/thyroxine concentrations during the neonatal period. A novel missense mutation with a transversion of G to A at position 1462 in exon 12 of the *DUOX2* gene that caused a replacement of glycine (G) with arginine (R) at codon 488 of the protein (c.1462G>A, p.[G488R]) was identified. One patient was a compound heterozygote for p.[L479SfsX3]+[G488R]. The other was homozygous for p.[G488R]. This p.G488R substitution occurred in a highly conserved glycine residue of the mammalian DUOX2 protein. The two patients had different haplotypes, suggesting that the p.G488R alleles were the result of independent, recurrent mutations. Later in life, both patients were still euthyroid even after discontinuing thyroid hormone therapy. We conclude that this p.G488R missense mutation in the *DUOX2* gene of the patients is associated with thyroid dysfunction that presents during the neonatal period.

**Keywords:** congenital hypothyroidism; dual oxidase 2 *(DUOX2)*; dyshormonogenesis; G488R mutation; neonatal screening.

***Corresponding author: Atsuko Yoshizawa-Ogasawara,** Okinaka Memorial Institute for Medical Research, 2-2-2 Toranomon, Minato-ku, Tokyo 105-8470, Japan,
E-mail: ayoshizawa-endo@umin.ac.jp
**Atsuko Yoshizawa-Ogasawara:** Department of Pediatrics, Ibaraki Children's Hospital, Mito, Japan
**Sayaka Ogikubo:** Okinaka Memorial Institute for Medical Research, Tokyo, Japan
**Mari Satoh:** Department of Pediatrics, Toho University Omori Medical Center, Tokyo, Japan
**Satoshi Narumi and Tomonobu Hasegawa:** Department of Pediatrics, Keio University School of Medicine, Tokyo, Japan

## Introduction

Congenital hypothyroidism (CH) occurs with an incidence of 1 in 4000 worldwide (1), while the incidence of CH in Japan currently ranges from 1 in 2200 to 1 in 2500 births (2). Neonatal screening programs for CH allow for early diagnosis and treatment. Lowering the bloodspot-thyrotropin (TSH) threshold to 10 mU/L has increased the ability of neonatal screening programs to detect hyperthyrotropinemia, which is characterized by elevated TSH levels and normal thyroxine ($T_4$) (2). The most common cause of CH, which accounts for up to 75%–80% of cases, is thyroid dysgenesis caused by aplasia, hypoplasia, or ectopic thyroid (3). Dyshormonogenesis accounts for the remaining 15%–20% of CH cases (3). Lifelong thyroid hormone replacement is usually required in cases of thyroid dyshormonogenesis. However, some patients can discontinue their medication after a period of replacement therapy.

Recent data from a study conducted in Italy (4) have shown that the percentage of defects associated with thyroid gland in situ cases has increased to 68%, and thyroid dysgenesis accounted for 32% of the CH cases with a bloodspot-TSH threshold of 12 or 10 mU/L. In a report from Japan, thyroid dysgenesis accounted for 63.2% of cases and dyshormonogenesis accounted for 36.8% of cases identified between 1981 and 1988 (2).

The recently identified gene mutations associated with CH that result in dyshormonogenesis involve dual oxidases (DUOXs), thyroid peroxidase (TPO), thyroglobulin (TG), sodium iodide symporter (NIS), pendrin (PDS) (1, 5), dual oxidase maturation factor 2 (DUOXA2) (6), and dehalogenase 1 (DEHAL1) (7). Biallelic mutations in the *TPO* gene can lead to total iodide organification defect (TIOD) when the resulting enzymatic impairment is severe (8–10). It has also been reported that some patients with TPO mutations exhibit partial iodide organification defect (PIOD) (10). Other candidate genes in which mutations lead to PIOD include *DUOX2* and *PDS*. Biallelic homozygous or compound heterozygous *DUOX2* mutations lead to goitrous CH (11–13), whereas monoallelic non-sense mutations cause transient CH (11, 14).

Here, we describe a novel p.G488R mutation in the *DUOX2* gene, identified in two unrelated Japanese patients with CH during a neonatal screening. One patient had a compound heterozygous mutation (p.[L479SfsX3]+[G488R]), while the other had a homozygous mutation (p.[G488R]+[G488R]); however, both were able to discontinue thyroid hormone therapy.

# Patients and methods

## Patients

Two patients from unrelated families were studied. These families were from different regions of Japan, and neither of the subjects had a family history of thyroid disease. The daily iodine intake (500–1000 μg) of the two patients and their mothers conformed to the nutritional standards of Japan, which averages 500–1500 μg/day (15, 16). Blood samples for the neonatal CH screening were collected within 5 days after birth. TSH levels were measured using blood filter papers. In cases where the TSH level was >10 mU/L, further examinations were performed. For the assessment of the permanence of hypothyroidism, L-$T_4$ administration is discontinued for 30 days at some point after the child reaches 3 years of age if no permanent cause of CH was found by scan or there was no TSH increase after the newborn period, as recommended by the American Academy of Pediatrics (AAP) (17). In more severely affected children, thyroid hormone replacement dosage is reduced by half. If the serum TSH value has not increased, then thyroid hormone treatment is discontinued for another 30 days with repeated serum free $T_4$ ($fT_4$) and TSH determination (17). In these two patients, thyroid function was reevaluated as per the AAP recommendation. Because perchlorate is not available for medical use in Japan, no perchlorate discharge test could be performed.

Patient 1, a child of a non-consanguineous couple, was delivered without complications after 38 weeks of gestation. Her TSH and $fT_4$ levels were 56.98 mU/L and 0.54 ng/dL, respectively, during the neonatal screening. During her first hospital visit, the patient's TSH level was 64.5 mU/L and her $T_4$ level was 4.5 μg/dL (Table 1). The core size of the patient's distal femur was 6 mm according to her X-ray. She received levothyroxine (L-$T_4$) supplementation (initial dose of 10 μg/kg/day). The patient's TSH level at neonatal screening was >50 mU/L, and a replacement dose of 3 μg/kg/day (45 μg/day) L-$T_4$ was still required when she was 3 years old owing to increased TSH levels. Therefore, a reassessment was performed after she entered elementary school. Because the replacement dose of L-$T_4$ was lowered to 1 μg/kg/day (25 μg/day) when she was 8 years old, L-$T_4$ treatment was discontinued for 30 days with repeated serum $fT_4$ and TSH determination. A soft, small thyroid was palpable for 3 years after she stopped taking the medication. The total volume of her thyroid gland was calculated as the sum of each lobe according to ultrasonography and measured 3.08 $cm^3$, a normal volume compared with that derived from healthy children with the same body height [mean (SD), 4.9 (1.1) $cm^3$]. A perchlorate discharge test was not performed. Her motor and mental development and her hearing were all normal. Her height and weight were 164 cm (+1.5 SD) and 61 kg (+1.4 SD), respectively, at 15 years of age, and her pubertal development was normal. Currently, her thyroid gland is not enlarged. The total volume of her thyroid gland is 12.1 $cm^3$ [mean (SD), 10.9 (2.5) $cm^3$] as measured by ultrasonography. She is still euthyroid (Table 1), and her urinary iodine level is 422 μg/L (Table 1). She attends high school and has no educational problems. Her mother has TSH and $fT_4$ levels of 1.37 mU/L and 0.98 ng/dL, respectively, at 49 years of age. Her father, at 52 years of age, has TSH and $fT_4$ levels of 0.727 mU/L and 1.00 ng/dL, respectively (Table 1).

Patient 2, the first child of a non-consanguineous couple, was delivered without complications after 40 weeks and 5 days of gestation. The patient's TSH level during the neonatal screening was >50 mU/L. During her first hospital visit, the patient's TSH and $fT_4$ levels were 165 mU/L and 0.3 ng/dL, respectively (Table 1). The patient's TG level then increased to 2350 ng/mL. The core size of her distal femur was 6 mm as measured by X-ray. L-$T_4$ treatment was initiated (10 μg/kg/day), and the patient's TG level decreased to 23.6 ng/mL 3 months later. Ultrasonography images indicated that her thyroid gland was in the proper location with a total volume of 1.7 $cm^3$ [mean (SD), 2.3 (0.7) $cm^3$]. The patient's motor and mental development and her hearing were all normal. Her TSH level was 165 mU/L at her first hospital visit, and the replacement dose of L-$T_4$ was still required at >5 μg/kg/day (70 μg/day) because of increased TSH at 3 years of age. Therefore, an attempt was made to discontinue the medication when she was 6 years old. However, she still required further replacement therapy because of her increased TSH level. After her replacement dose was lowered to 0.75 μg/kg/day (25 μg/day), L-$T_4$ treatment was then discontinued at 12 years of age. A perchlorate discharge test was not performed, and urinary iodine was not examined. At 12 years of age, her height and weight were 145 cm (−0.2 SD) and 35 kg (−0.2 SD), respectively. She is currently euthyroid (Table 1). She attends junior high school and has no educational problems. Her pubertal development is normal, and her younger brother tested negative for CH during his neonatal screening. Her mother, who is in her 30 s, has TSH and $fT_4$ levels of 1.57 mU/L and 1.07 ng/dL, respectively (Table 1). It is currently not possible to study thyroid function and gene analysis in other family members.

## Laboratory tests

TSH levels were measured using an electrochemiluminescence immunoassay (ECLIA) (Architect; Abbott, Wiesbaden, Germany), with a reference range of 0.50–5.00 mU/L. $FT_4$ (0.90–1.70 ng/dL) (Architect, Abbott), $T_4$ (6.10–12.4 μg/dL) (Elecsys $T_4$ II; Roche Diagnostics, Mannheim, Germany), and TG (<6 months old, <95 ng/mL; >6 months old, <32.7 ng/mL) (Elecsys Tg, Roche Diagnostics) levels were also measured using an ECLIA. According to X-rays, the core size of the distal femur was measured, with a reference range of 4.1 to 9.7 mm for babies born after 37 weeks of gestation (18). The total volume of the thyroid gland was calculated using ultrasonography, with a reference range derived from healthy children with the same body height (19). The concentration of urinary iodine was measured using colorimetry (median 262 μg/L) (Iodine Monit; Hitachi Chemical, Tokyo, Japan).

## DNA sequence analysis

Genomic DNA was isolated from peripheral blood lymphocytes. All exons of the *DUOX2* gene were amplified by polymerase chain reaction (PCR) using primers described in previous studies (11). The

| | Reference values | Patient 1 | Patient 2 |
|---|---|---|---|
| Sex | | Female | Female |
| Family history | | – | – |
| Deafness | | – | – |
| Neonatal screening | | | |
| Age, day | | 5 | 5 |
| TSH, mU/L | <10 | 56.98 | >50 |
| $fT_4$, ng/dL | 0.90–1.70 | 0.54 | NA |
| First visit | | | |
| Age | | 1 month | 13 days |
| TSH, mU/L | 0.50–5.00 | 64.5 | 165 |
| $fT_4$, ng/dL | 0.90–1.70 | NA | 0.3 |
| $T_4$, μg/dL | 6.10–12.4 | 4.5 | 1.8 |
| Recent data | | | |
| Age, years | | 17 | 14 |
| TSH, mU/L | 0.50–5.00 | 2.33 | 4.32 |
| $fT_4$, ng/dL | 0.90–1.70 | 0.95 | 1.10 |
| TG, ng/mL | <32.7 | 57.1 | 37.2 |
| L-$T_4$ therapy | | – | – |
| Age at $T_4$ withdrawal, years | | 8 | 12 |
| Urinary iodine, μg/L | Median, 262 | 422 | NA |
| Gene, Genotype | | *DUOX2*, p.[L479SfsX3]+[G488R] | *DUOX2*, p.[G488R]+[G488R] |
| Mother | | | |
| Age, years | | 49 | 30s |
| TSH, mU/L | 0.50–5.00 | 1.37 | 1.57 |
| $fT_4$, ng/dL | 0.90–1.70 | 0.98 | 1.07 |
| Gene, Genotype | | *DUOX2*, p.[L479SfsX3] | *DUOX2*, p.[G488R] |
| Father | | | |
| Age, years | | 52 | NA |
| TSH, mU/L | 0.50–5.00 | 0.72 | NA |
| $fT_4$, ng/dL | 0.90–1.70 | 1.00 | NA |
| Gene, Genotype | | *DUOX2*, p.[G488R] | NA |

**Table 1** Clinical, biochemical, and genetic data.
TSH, thyrotropin; $fT_4$, free thyroxine; $T_4$, thyroxine; TG, thyroglobulin; L-$T_4$, levothyroxine; NA, not available.

purified PCR products were directly sequenced using an automated DNA sequence analyzer (ABI 3130*xl*; Applied Biosystems, Foster City, CA, USA). The PCR products containing *DUOX2* mutations were subcloned to pCR2.1 vectors using a TA-cloning kit (Invitrogen, San Diego, CA, USA) to determine the specific changes in the nucleotide sequence. Transformation of the products was performed according to the manufacturer's instructions. As for patients harboring mutations in DUOX2, we also sequenced the other genes implicated in CH, including *TSHR*, *PAX8*, *NKX2.1*, *NKX2.5*, *FOXE1*, *TPO*, *TG*, *NIS*, *PDS*, *DUOXA2*, and *DEHAL1* using the MiSeq instrument (Illumina Inc., San Diego, CA, USA) according to the SureSelect protocol (Agilent Technologies, Santa Clara, CA, USA). Briefly, 3 μg of genomic DNA was used for the SureSelect capture method. Exons of the 97 known genes associated with congenital endocrine disorders (including 11 CH-related genes) were identified in the University of California Santa Cruz table browser (http://genome.ucsc.edu/). In total, we targeted 902 regions comprising 200,675 bp using the SureSelect method. DNA obtained from SureSelect solution-based sequence capture was subjected to MiSeq sequencing according to the manufacturer's protocol. This study was approved by the Ethics Committees at Ibaraki Children's Hospital, Toho University, and Okinaka Memorial Institute for Medical Research. Written informed consent was obtained from the parents of the subjects.

# Results

## Molecular analysis

Direct sequencing of the genomic DNA revealed that patient 1 had a biallelic compound heterozygous mutation in the *DUOX2* gene. One was a novel missense mutation with a transversion of G to A at 1462 in exon 12 that replaced glycine (G) with arginine (R) at codon 488 (c.1462G>A, p.[G488R]) (Figure 1A). The other mutation was a deletion-insertion mutation in exon 12 of the *DUOX2* gene where AG replaced the nucleotide sequence of CTATCC at base pairs 1435–1440. This deletion-insertion

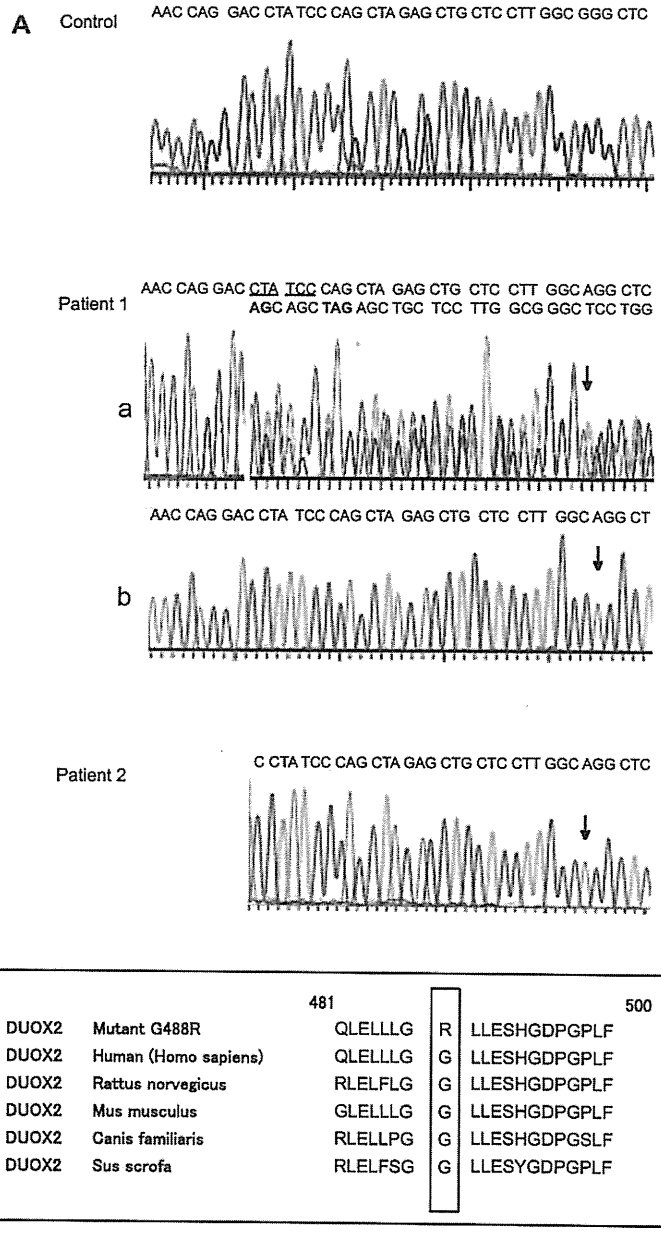


**Figure 1** (A) Sequencing chromatograms of DUOX2 exon 12 from a control subject, patient 1, and patient 2. The arrows indicate the position of the monoallelic or biallelic G to A mutation (c.1462G>A). Patient 1 is heterozygous for a deletion of CTATCC (underlined) and an insertion of AG (bold) at position 1435–1440. The deletion-insertion leads to a frameshift producing a stop codon at amino acid 481 (bold) (a). In one allele, the sequence after TA cloning indicates a transversion of G to A at position 1462, resulting in a monoallelic p.G488R mutation (b). Patient 2 has a biallelic G to A mutation. (B) Analysis of DUOX2 protein homology among different species. The glycine residue mutated to arginine (p.G488R) in the patients is highly conserved in mammalian DUOX2 proteins.

leads to a frameshift producing a stop at codon 481 (c.1435_1440delCTATCCinsAG, p.[L479SfsX3]) (Figure 1A). The unaffected mother of patient 1 had a monoallelic mutation p.[L479SfsX3], and the unaffected father of patient 1 had a monoallelic mutation p.[G488R] (Table 1).

Patient 2 had a biallelic mutation p.[G488R]+[G488R] in the *DOUX2* gene (Figure 1A). After obtaining written informed consent, a gene analysis of the mother of patient 2 was performed and a monoallelic mutation p.[G488R] was identified in the *DUOX2* gene (Table 1).

This novel p.G488R substitution occurred in a highly conserved glycine residue of the mammalian DUOX2 protein (Figure 1B) and was not detected in the 100 alleles analyzed from 50 additional control subjects. The

deletion-insertion mutation p.[L479SfsX3] was reported in 2008 (20). Neither one of the patients had any additional mutations of TSHR, PAX8, NKX2.1, NKX2.5, FOXE1, TPO, TG, NIS, PDS, DUOXA2, or DEHAL1 except for a previously reported TG polymorphism (Reference SNP Cluster Report: rs2076737).

## Founder effect

We identified two unrelated patients who also had the novel p.G488R mutation. To distinguish whether the recurrent p.G488R alleles were derived from a common ancestral allele or occurred independently, we analyzed 12 single nucleotide polymorphisms (SNPs) within the coding region of the *DUOX2* gene (Table 2). The patients with the p.G488R mutation had different haplotypes, suggesting that the p.G488R alleles were the result of independently occurring mutations.

# Discussion

The mutated CH genes resulted in defective thyroid hormone synthesis that has recently been identified to include the *DUOXs*, *TPO*, *TG*, *NIS*, *PDS* (1, 5), *DUOXA2* (6), and *DEHAL1* (7) genes. A decrease in hydrogen peroxidase ($H_2O_2$) generation due to *DUOX2* gene mutations has been recognized as one cause of thyroid dyshormonogenesis (11). Other cases of CH caused by *DUOX2* gene mutations in infants have also been identified (12–14). In Japan, novel mutations in the *DUOX2* gene were detected in eight Japanese patients with transient CH (20) and one Japanese adult patient with a dyshormonogenic goiter (21). Moreover, Grasberger et al. (22), Tonacchera et al. (23), and Hoste et al. (24) have also recently published functional studies of novel DUOX2 mutations.

| Exon | cDNA | Nucleotide | Frequency in control subjects | G488R | |
|---|---|---|---|---|---|
| | | | | Patient 1 | Patient 2 |
| 3 | 303 | C, A | 95; 5 | CC | CC |
| 4 | 413 | C, T | 11; 89 | TT | TT |
| 5 | 558 | C, T | 48; 52 | CT | CT |
| | 567 | C, T | 46; 54 | CT | TT |
| | 597 | G, C | 46; 54 | GC | GC |
| | 598 | G, A | 46; 54 | GA | GA |
| | 633 | C, T | 46; 54 | CT | CT |
| 12 | 1461 | G, C | 4; 96 | CC | CC |
| 16 | 2033 | A, G | 93; 7 | AA | AA |
| 24 | 3200 | C, T | 15; 85 | TT | TT |
| 29 | 3966 | C, T | 96; 4 | CC | CC |
| 32 | 4479 | C, G | 95; 5 | CC | CC |

**Table 2** Twelve SNPs in patients with G488R mutation.

The p.G488R mutation in the *DUOX2* gene has not been previously reported and was also not detected in 100 alleles from control subjects. The glycine residue is highly conserved in mammalian *DUOX2* genes, and neither patient had additional mutations in the other candidate genes that could cause CH. Therefore, this mutation is the probable cause of hypothyroidism in these two patients.

To evaluate whether this mutation was inherited from a common ancestral chromosome or an independently occurring mutation in a heterogeneous genetic background, we studied 12 SNPs within the coding region of the *DOUX2* gene. The SNPs of p.G488R alleles were not identical, suggesting that the p.G488R mutation is an independently occurring mutation.

The *DUOX2* gene is localized to chromosome 15q15.3 and consists of 33 exons encoding an mRNA that is 6376 nucleotides in length (25, 26). The encoded protein is a 1548-amino-acid polypeptide that includes a 26-amino-acid signal peptide. The DUOX2 protein localizes to the apical membrane of thyrocytes and is involved in the $Ca^{2+}$/reduced nicotinamide adenine dinucleotide phosphate-dependent generation of $H_2O_2$ (27). TPO requires $H_2O_2$ to catalyze both the iodination of tyrosine residues and the coupling of iodotyrosine residues on TG (28).

In reports describing the functional analysis of *DUOX2* gene mutations, the Q36H and R376W mutations completely abolished DUOX2 function (22). The D506N mutation displayed a partial deficiency phenotype with a reduction in the surface expression of a mutant protein with normal intrinsic activity that is involved in the generation of $H_2O_2$ (22). S911L and C1052Y mutations caused a partial defect in the $H_2O_2$-generating system and caused reduced expression of DUOX2 at the cell surface (23). Moreover, the G1518S mutation abolished protein activity despite expression at the cell surface (24). G488R localizes to the extracellular region of DUOX2, which contains a TPO-like domain. This suggests that the G488R mutation likely results in a partial impairment of function, although the expression of the mutant protein has not yet been studied.

Previously, Varela et al. (13) and Chiesa et al. (29) reported *DUOX2* gene mutations in three Argentinean patients with CH. One patient was a compound heterozygote for p.[Q36H]+[S965fsX994], and his perchlorate discharge test result (46%) at 5 years of age (reference value, <10%) indicated PIOD. Two siblings in another family who were